

The Nucleon Anapole Form Factor in Chiral Perturbation Theory to Sub-leading Order

C.M. Maekawa¹, J. S. Veiga² and U. van Kolck³

*Kellogg Radiation Laboratory, 106-38
California Institute of Technology
Pasadena, CA 91125*

Abstract

The anapole form factor of the nucleon is calculated in chiral perturbation theory to sub-leading order. This is the lowest order in which the isovector anapole form factor does not vanish. The anapole moment depends on counterterms that reflect short-range dynamics, but the momentum dependence of the form factor is determined by pion loops in terms of parameters that could in principle be fixed from other processes. If these parameters are assumed to have natural size, the sub-leading corrections do not exceed $\sim 30\%$ at momentum $Q \sim 300$ MeV.

¹maekawa@krl.caltech.edu

²jaime@krl.caltech.edu

³vankolck@krl.caltech.edu

Parity-violating electron scattering has long played a role in understanding electroweak interactions, and has more recently been explored as a tool for the study of nucleon structure. The SAMPLE collaboration has carried out electron scattering measurements at a momentum transferred of $Q^2 = 0.1 \text{ MeV}^2$ on both the proton [1] and the deuteron [2], for a simultaneous extraction of the strange magnetic (G_M^s) and the axial form factor of the nucleon (G_A^e).

One quantity that contributes in electron scattering as G_A^e is the anapole form factor, which is an extension for $Q^2 > 0$ of the anapole moment. The anapole is a parity-violating electromagnetic moment of a charge particle with spin [3]. Recently the effect of the nuclear anapole moment in atomic parity violation was measured precisely in ^{133}Cs transitions [4], and a discrepancy with theory found. Parity violation in this case is enhanced by nuclear medium effects. No such enhancement is present in parity-violating electron scattering off the proton and deuteron; however, the anapole form factor could still be visible. Using previous estimates of the anapole moment [5, 6], the proton data implies a positive value for G_M^s [1], in disagreement with most theoretical predictions (for a summary, see Ref. [7]).

Experiments of current interest [1, 2, 8, 9, 10] are performed at finite $Q^2 = -q^2$. For $Q < M_{QCD}$, where $M_{QCD} \sim 1 \text{ GeV}$ is the characteristic QCD mass scale, we are deep in the non-perturbative regime of QCD, where currently the only possible systematic calculations are in terms of hadrons. At $Q \sim O(m_\pi)$ the photon can resolve the pion cloud around the non-relativistic nucleon, and calculations are possible in Chiral Perturbation Theory (ChPT), which involves pions, nucleons, and delta isobars, and which has been successfully applied to hadronic and nuclear systems [11, 12]. The first anapole calculations were limited to $Q^2 = 0$ in leading [5, 6] and sub-leading orders [6, 13]. Recently, the full form factor of the nucleon was calculated in leading order [14, 15]. In this order the form factor comes entirely from the pion cloud and is purely isoscalar, while experiments are most sensitive to the isovector component [7]. Here we report results of sub-leading contributions to the nuclear anapole form factor, where the isovector part first appears.

In the framework of ChPT, QCD symmetries are used as a guide to build the most general effective Lagrangian. The number of terms in the Lagrangian is not constrained by symmetries, which demands a power counting argument to order interactions according to the expected size of their contributions. In order to fulfill chiral symmetry requirements, pions couple derivatively in the chiral limit; this derivative coupling brings to the amplitude powers of pion momentum or powers of the delta-nucleon mass difference (comparable to the pion mass). Chiral symmetry breaking terms involve quark masses, so they bring into the amplitude powers of the pion mass. Thus one has a chiral index (Δ) available to order the Lagrangian terms, $\mathcal{L} = \sum_{\Delta} \mathcal{L}^{(\Delta)}$. For strong interactions, the index counts powers of Q/M_{QCD} , and it is given by $\Delta = d + n/2 - 2$, where n is the number of fermions fields and d counts the numbers of derivatives, powers of the pion mass, and of the delta-nucleon mass difference. In the presence of electromagnetic interactions, it is convenient to include in d powers of the charge e as well. Weak interactions, on the other hand, bring powers of a very small factor $G_F f_\pi^2$, where G_F is the Fermi constant and f_π the pion decay constant. Since we count these factors explicitly, negative indices appear.

Based on this power counting argument the interactions relevant to our problem are the following. The parity-conserving terms are well known [11]:

$$\mathcal{L}_{str/em}^{(0)} = \frac{1}{2} (D_\mu \boldsymbol{\pi})^2 - \frac{1}{2} m_\pi^2 \boldsymbol{\pi}^2 + \bar{N} i v \cdot D N - \frac{g_A}{f_\pi} \bar{N} (\boldsymbol{\tau} \cdot S \cdot D \boldsymbol{\pi}) N + \dots \quad (1)$$

$$\begin{aligned} \mathcal{L}_{str/em}^{(1)} &= \frac{1}{4m_N} \bar{N} [(v \cdot D)^2 - D^2] N + i \frac{g_A}{2m_N f_\pi} \bar{N} \{S \cdot D, \boldsymbol{\tau} \cdot v \cdot D \boldsymbol{\pi}\} N \\ &\quad - \frac{i}{4m_N} \bar{N} [S^\mu, S^\nu] [1 + \kappa^s + (1 + \kappa^v) \tau_3] N F_{\mu\nu} + \dots \end{aligned} \quad (2)$$

Here $\boldsymbol{\pi}$ denotes the pion field with $f_\pi = 93$ MeV the pion decay constant; N represents the heavy nucleon field of four-velocity v^μ and spin S^μ (in the nucleon rest frame $v^\mu = (1, \vec{0})$ and $S^\mu = (0, \vec{\sigma}/2)$); A_μ is the photon field and $F_{\mu\nu}$ is the photon strength field; $D_\mu = (\partial_\mu - ieQ A_\mu)$ is the covariant derivative, with $Q_{ab}^{(\pi)} = -i\varepsilon_{3ab}$ for a pion and $Q^{(N)} = (1 + \tau_3)/2$ for a nucleon; and “...” stands for other interactions with more pions, nucleons and deltas. The pion-nucleon coupling g_A and the magnetic photon-nucleon couplings $\kappa^{(s)}$ and $\kappa^{(v)}$ are not determined from symmetry but expected to be $O(1)$; indeed, one finds $g_A = 1.267$, $\kappa^{(s)} = -0.12$, and $\kappa^{(v)} = 5.62$ [11].

The relevant parity-violating terms were discussed in Ref. [6]:

$$\mathcal{L}_{weak}^{(-1)} = -\frac{h_{\pi NN}^{(1)}}{\sqrt{2}} \bar{N} (\boldsymbol{\tau} \times \boldsymbol{\pi})_3 N + \dots \quad (3)$$

$$\begin{aligned} \mathcal{L}_{weak}^{(0)} &= -\frac{2}{f_\pi^2} \bar{N} S^\mu \left\{ \left(h_A^{(1)} + h_A^{(2)} \tau_3 \right) \left[(\boldsymbol{\pi} \times \partial_\mu \boldsymbol{\pi})_3 + e A_\mu (\boldsymbol{\pi}^2 - \pi_3^2) \right] \right. \\ &\quad \left. + h_A^{(2)} (\boldsymbol{\pi} \times \boldsymbol{\tau})_3 \partial_\mu \pi_3 \right\} N \\ &\quad + \frac{1}{f_\pi} \bar{N} \left[\left(h_V^{(0)} + \frac{4}{3} h_V^{(2)} \right) \frac{1}{2} \boldsymbol{\tau} \cdot v \cdot D \boldsymbol{\pi} - 2 h_V^{(2)} \tau_3 v \cdot D \pi_3 \right] N + \dots \end{aligned} \quad (4)$$

$$\mathcal{L}_{weak}^{(2)} = \frac{2}{m_N^2} \bar{N} (\tilde{a}_0 + \tilde{a}_1 \tau_3) S_\mu N \partial_\nu F^{\mu\nu} + \dots \quad (5)$$

Here $h_{\pi NN}^{(1)}$, $h_A^{(1,2)}$ and $h_V^{(0,2)}$ are, respectively, Yukawa, axial-vector and vector parity-violating pion-nucleon couplings, with superscripts referring to isospin $\Delta I = 0, 1$ and 2 . On the basis of naive dimensional analysis, $h_{\pi NN}^{(1)} f_\pi \sim O(G_F f_\pi^2 M_{QCD})$, and $h_A^{(1,2)} \sim h_V^{(0,2)} \sim O(G_F f_\pi^2)$. Also, $\tilde{a}_{0,1}$ are short-range contributions to the anapole moment, expected to be of $O(e G_F f_\pi^2 / m_N^2) = O(e G_F / (4\pi)^2)$.

The current-current electron-nucleon interaction has the form

$$iT = -ie \bar{e}(k') \gamma^\mu e(k) D_{\mu\nu}(q) \bar{N}(p') J_{an}^\nu(q) N(p), \quad (6)$$

where $e(k)$ ($N(p)$) is an electron (nucleon) spinors of momentum k (p), $-e$ is the electron charge, $iD_{\mu\nu}(q) = -i\eta_{\mu\nu}/q^2$ is the photon propagator with $q^2 = (p - p')^2 \equiv -Q^2 < 0$, and the nucleon anapole current iJ_{an}^μ reads

$$J_{an}^\mu(q) = \frac{2}{m_N^2} \left[a_0 F_A^{(0)}(-q^2) + a_1 F_A^{(1)}(-q^2) \tau_3 \right] (S^\mu q^2 - S \cdot q q^\mu), \quad (7)$$

where a_0 and a_1 are the isoscalar and isovector anapole moments, and $F_A^{(0)}(-q^2)$ and $F_A^{(1)}(-q^2)$ their corresponding form factors.

The diagrams contributing to the nucleon anapole form factor in next-to-leading order (NLO) are shown in Figs. 1,2,3. We classify them according to the combination of couplings that appear.

The NLO diagrams of Fig. 1 are built from the leading interactions in $\mathcal{L}_{str/em}^{(0)}$ and $\mathcal{L}_{weak}^{(-1)}$, plus one insertion of an operator from $\mathcal{L}_{str/em}^{(1)}$. This insertion can be (i) a kinetic correction—either in the nucleon propagator or in the external energy—to the leading order (LO) diagrams computed in Ref. [15]; or (ii) a sub-leading (magnetic) photon-nucleon interaction. The size of these diagrams is $O(eG_F Q^2/(4\pi)^2)$. Indeed, LO contributions are $O(eG_F M_{QCD} Q/(4\pi)^2)$ [15], and NLO is of relative size $O(Q/M_{QCD})$. (For example, the diagram 1e has a kinetic insertion of Q^2/m_N and an extra propagator $1/Q$ compared to the corresponding LO diagram.) Diagrams (c), (g) and (j) do not contribute to the anapole form factor because they are proportional to v^μ and the diagram (d) vanishes because it is proportional to $S \cdot v = 0$. Diagram (i) gives a pure isovector contribution, but it gets cancelled by the isovector part of diagram (k). Therefore, the sum of all diagrams in Fig. 1 is a purely isoscalar result.

The diagrams in Fig. 2 have axial-vector vertices from $\mathcal{L}_{weak}^{(0)}$. They have both isovector and isoscalar parts. To evaluate the size of the contributions represented by these diagrams, one takes, for example, the diagram 2a: it has a parity-violating two pion-nucleon axial vertex of the order $G_F Q$, a photon-pion vertex of $O(eQ)$, two pion propagators each one of $O(1/Q^2)$, and the loop integration of $O(Q^4/(4\pi^2))$. Diagrams of this type are then also of $O(eG_F Q^2/(4\pi)^2)$.

In Fig. 3, diagrams contain vector couplings coming from $\mathcal{L}_{weak}^{(0)}$. Since the parity-violating vector coupling is $O(Q/M_{QCD})$ smaller than the LO Yukawa coupling, these contributions are clearly also $O(eG_F Q^2/(4\pi)^2)$. Diagrams (b) and (d) are proportional to v^μ and do not contribute to the anapole form factor. Diagrams (a) and (c) give a purely isovector contribution.

Finally, there are short range contributions from $\mathcal{L}_{weak}^{(2)}$ depicted in Fig. 4. From the size of $\tilde{a}_{0,1}$, we see that these contributions are also $O(eG_F Q^2/(4\pi)^2)$.

Note that to this order there are no contributions from the delta isobar [13]. Deltas would contribute at this order through intermediate states of diagrams with one pion loop, e.g. diagram 1c with one nucleon propagator replaced by a delta: at least there would be one $\pi N \Delta$ vertex, either parity conserving or violating, and both kinds of vertices have the same $i\gamma_5$ structure, which vanishes in the framework of ChPT. The first non-vanishing delta contribution shows up in an order higher than we are considering here.

Let us first discuss the isoscalar component, which did not vanish in leading order [15],

$$a_0^{LO} = \frac{eg_A h_{\pi NN}^{(1)} m_N^2}{48\sqrt{2}\pi f_\pi m_\pi}. \quad (8)$$

As the final contribution represented by the diagrams in Fig. 1 is isoscalar, we add it to the isoscalar contribution of the diagrams in Fig. 2, and find for the anapole moment in

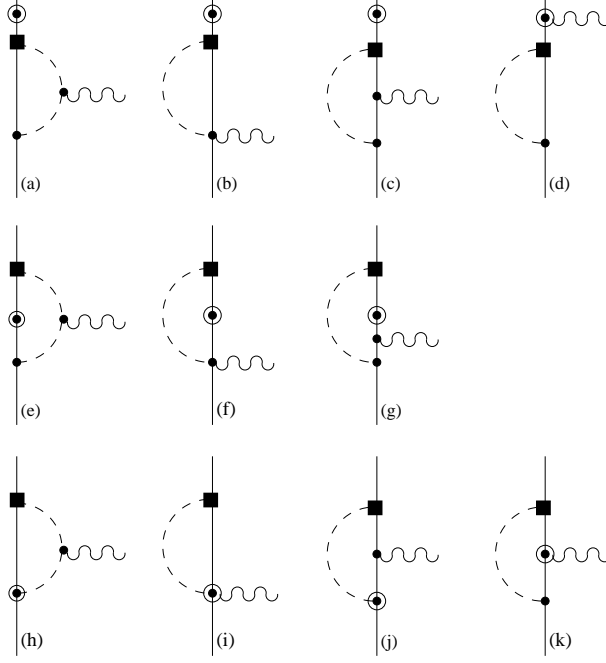


Figure 1: Diagrams contributing to the nucleon anapole form factor in sub-leading order coming from one insertion of an $\mathcal{L}_{str/em}^{(1)}$ operator. Solid, dashed and wavy lines represent nucleon, pions and (virtual) photons, respectively; squares represent the parity-violating vertex from $\mathcal{L}_{weak}^{(-1)}$; single filled circles stand for interactions from $\mathcal{L}_{str/em}^{(0)}$ and double circles represent interactions from $\mathcal{L}_{str/em}^{(1)}$. For simplicity only one possible orderings are shown here.

next-to-leading order,

$$a_0^{NLO} = \tilde{a}_0(\mu) + \frac{em_N^2}{(4\pi)^2 f_\pi^2} \left(-\frac{g_A h_{\pi NN}^{(1)} f_\pi}{\sqrt{2} m_N} + \frac{h_A^{(1)}}{3} \right) \ln \left(\frac{\mu^2}{m_\pi^2} \right), \quad (9)$$

with

$$\begin{aligned} \tilde{a}_0(\mu) = \tilde{a}_0 + \frac{em_N^2}{(4\pi)^2 f_\pi^2} & \left[\left(-\frac{g_A h_{\pi NN}^{(1)} f_\pi}{\sqrt{2} m_N} + \frac{h_A^{(1)}}{3} \right) \left(\frac{1}{\varepsilon} + 1 - \gamma + \ln 4\pi \right) \right. \\ & \left. - \frac{1}{3} \left(-\frac{g_A h_{\pi NN}^{(1)} f_\pi}{\sqrt{2} m_N} + \frac{2h_A^{(1)}}{3} \right) \right], \end{aligned} \quad (10)$$

where μ is the renormalization scale and $\gamma = 0.5772157$ is the Euler constant. As usual in ChPT, the only term that can be calculated explicitly is non-analytic in the pion mass; it has the expected size, that is, it is $O(m_\pi/M_{QCD})$ smaller than a_0^{LO} . This result for the

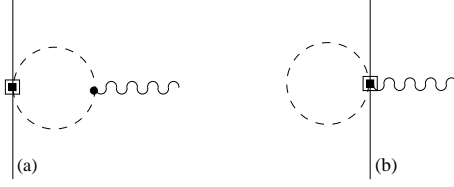


Figure 2: Diagrams contributing to the nucleon anapole form factor in sub-leading order coming from one insertion of the axial-vector couplings in $\mathcal{L}_{weak}^{(0)}$, represented by a double square. Other symbols are as in Fig. 1.

anapole moment agrees with that of a previous calculation [13]. The term in $h_A^{(1)}$ agrees with Ref. [6].

The total isoscalar form factor reads

$$F_0^{LO+NLO}(Q^2) = 1 + \frac{a_0^{LO}}{(a_0^{LO} + a_0^{NLO})} [F_0^{LO}(Q^2) - 1] + \frac{1}{(a_0^{LO} + a_0^{NLO})} \frac{em_N^2}{3(4\pi f_\pi)^2} \left\{ \frac{g_A h_{\pi NN}^{(1)} f_\pi}{\sqrt{2} m_N} [F^{NLO1}(Q^2) - 1] - \frac{2h_A^{(1)}}{3} [F^{NLO2}(Q^2) - 1] \right\} \quad (11)$$

where $F_0^{LO}(Q^2)$ is the leading-order form factor given by [15]

$$F_0^{LO}(Q^2) = \frac{3}{2} \left\{ -\left(\frac{2m_\pi}{\sqrt{Q^2}}\right)^2 + \left[\left(\frac{2m_\pi}{\sqrt{Q^2}}\right)^2 + 1 \right] \frac{2m_\pi}{\sqrt{Q^2}} \arctan \frac{\sqrt{Q^2}}{2m_\pi} \right\}, \quad (12)$$

$F^{NLO1}(Q^2)$ comes from the diagrams in Fig. 1,

$$F^{NLO1}(Q^2) = -3 \left[\left(\frac{2m_\pi}{Q}\right)^2 + 2 \right] \left[1 - \frac{1}{2} \sqrt{1 + \left(\frac{2m_\pi}{Q}\right)^2} \ln \frac{\sqrt{1 + \left(\frac{2m_\pi}{Q}\right)^2} + 1}{\sqrt{1 + \left(\frac{2m_\pi}{Q}\right)^2} - 1} \right], \quad (13)$$

and $F^{NLO2}(Q^2)$ comes from the diagrams in Fig. 2,

$$F^{NLO2}(Q^2) = -3 \left[\left(\frac{2m_\pi}{Q}\right)^2 + 1 \right] \left[1 - \frac{1}{2} \sqrt{1 + \left(\frac{2m_\pi}{Q}\right)^2} \ln \frac{\sqrt{1 + \left(\frac{2m_\pi}{Q}\right)^2} + 1}{\sqrt{1 + \left(\frac{2m_\pi}{Q}\right)^2} - 1} \right]. \quad (14)$$

As in lowest order, the momentum dependence is fixed by the pion cloud, and therefore the scale for momentum variation is determined by $2m_\pi$. Because there are several

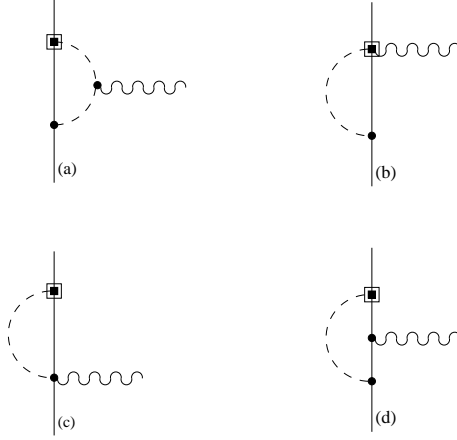


Figure 3: Diagrams contributing to the nucleon anapole form factor in sub-leading order coming from one insertion of the vector couplings in $\mathcal{L}_{weak}^{(0)}$, represented by a double square. Other symbols are as in Fig. 1. For simplicity only one of two possible orderings are shown here.

contributions to the form factor, for which we follow the conventional normalization to 1, the exact form depends also on the coupling constants that contribute to the anapole moment. Unfortunately these are currently not well determined by other data; once they are, one can plot the form to this order. Here we can only study “reasonable” estimates of the momentum dependence. Assuming [6] $\tilde{a}_0(\Lambda_{\chi SB}) = 0$ where $\Lambda_{\chi SB} \sim 4\pi f_\pi$ is the chiral symmetry breaking scale, we rewrite

$$F_0^{LO+NLO}(Q^2) \simeq F_0^{LO}(Q^2) + \frac{3m_\pi}{\pi m_N} (1-r) \ln \left(\frac{\Lambda_{\chi SB}^2}{m_\pi^2} \right) [F_0^{LO}(Q^2) - 1] \\ + \frac{m_\pi}{\pi m_N} \left\{ [F^{NLO1}(Q^2) - 1] - 2r [F^{NLO2}(Q^2) - 1] \right\}, \quad (15)$$

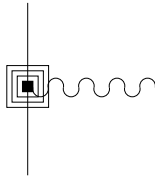


Figure 4: Diagram contributing to the nucleon anapole moment in sub-leading order coming from $\mathcal{L}_{weak}^{(2)}$, represented by a quadruple square. Other symbols are as in Fig. 1.

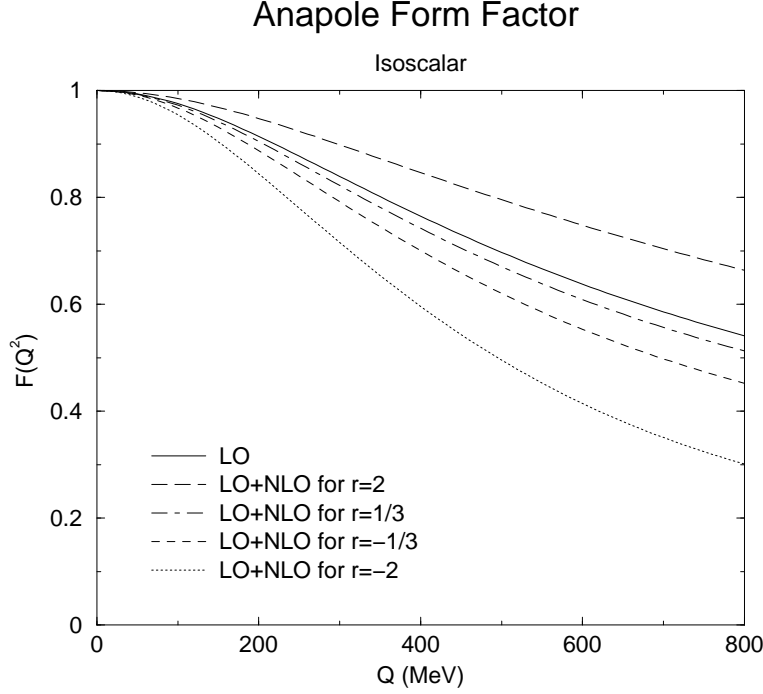


Figure 5: The isoscalar anapole form factor F_0 as function of Q in χ PT: leading order (LO) and next-to-leading order (NLO) for a few reasonable values of parameters expressed by the ratio $r = \sqrt{2}m_N h_A^1 / 3g_A f_\pi h_{\pi NN}^1$.

where $r = \sqrt{2}m_N h_A^{(1)} / 3g_A f_\pi h_{\pi NN}^{(1)} \sim 1/3$. In Fig. 5 we show $F_0^{LO}(Q^2)$ and $F_0^{LO+NLO}(Q^2)$ for several values of r .

From the form factor is easy to extract closed forms for the mean square radius. We find

$$\langle r_0^2 \rangle^{LO+NLO} = \frac{3}{10m_\pi^2} \frac{1}{(a_0^{LO} + a_0^{NLO})} \left[a_0^{LO} - \frac{2em_N^2}{3(4\pi f_\pi)^2} \left(\frac{4g_A h_{\pi NN}^{(1)} f_\pi}{\sqrt{2}m_N} - h_A^{(1)} \right) \right], \quad (16)$$

Using the same estimates as for the form factor,

$$\langle r_0^2 \rangle^{LO+NLO} \simeq \frac{3}{10m_\pi^2} \left[1 + \frac{6m_\pi}{\pi m_N} (1-r) \left(\ln \frac{\Lambda_{\chi SB}}{m_\pi} - 1 \right) - \frac{2m_\pi}{\pi m_N} \right]. \quad (17)$$

For r ranging from -2 to 2 , $\langle r_0^2 \rangle^{LO+NLO}$ ranges from 3 to $1 \times 10^{-5} \text{ MeV}^{-2}$.

The isovector anapole moment a_1^{NLO} comes from contributions represented by the diagrams in Figs. 2,3. We find

$$a_1^{NLO} = \frac{em_N^2}{6(4\pi f_\pi)^2} \left[2h_A^{(2)} + g_A \left(h_V^{(0)} + \frac{4}{3}h_V^{(2)} \right) \right] \ln \left(\frac{\mu^2}{m_\pi^2} \right) + \tilde{a}_1(\mu), \quad (18)$$

where

$$\tilde{a}_1(\mu) = \tilde{a}_1 + \frac{em_N^2}{6(4\pi f_\pi)^2} \left[2h_A^{(2)} + g_A \left(h_V^{(0)} + \frac{4}{3}h_V^{(2)} \right) \right] \left(\frac{1}{\varepsilon} + 1 - \gamma - \frac{2}{3} + \ln 4\pi \right). \quad (19)$$

Again, our result has the expected size and agrees with Ref. [13]. The term in $h_A^{(2)}$ agrees with Ref. [6].

Contrary to the isoscalar part, the isovector anapole form factor first appears in next-to-leading order and reads

$$F_1^{NLO}(Q^2) = 1 - \frac{em_N^2}{9(4\pi f_\pi)^2} \frac{1}{a_1^{NLO}} \left[2h_A^{(2)} + g_A \left(h_V^{(0)} + \frac{4}{3}h_V^{(2)} \right) \right] [F^{NLO2}(Q^2) - 1]. \quad (20)$$

Again, for illustration we consider some representative values of $\tilde{a}_1(\mu)$: $\tilde{a}_1(\Lambda_{\chi SB}) = 0$, $\tilde{a}_1(\Lambda_{\chi SB}) = -2\alpha \ln \left(\frac{\Lambda_{\chi SB}^2}{m_\pi^2} \right)$, $\tilde{a}_1(550 \text{ MeV}) = 0$, $\tilde{a}_1(550 \text{ MeV}) = -2\alpha \ln \left(\frac{(550 \text{ MeV})^2}{m_\pi^2} \right)$, with $\alpha = \frac{em_N^2}{6(4\pi f_\pi)^2} \left[2h_A^{(2)} + g_A \left(h_V^{(0)} + \frac{4}{3}h_V^{(2)} \right) \right]$ and they all are summarized as

$$F_1(Q^2) \simeq 1 + s \frac{2}{3} \ln^{-1} \left(\frac{\mu^2}{m_\pi^2} \right) [F^{NLO2}(Q^2) - 1], \quad (21)$$

where $s = -1$ for $\tilde{a}_1(\mu) = 0$ and $s = 1$ for $\tilde{a}_1(\mu) = -2\alpha \ln(\mu^2/m_\pi^2)$, $\mu = 0.55, 1.2 \text{ GeV}$. Fig. 6 shows $F_1^{NLO}(Q^2)$ for these four cases of s and μ .

The isovector mean square radius is

$$\langle r_1^2 \rangle^{NLO} = \frac{1}{10m_\pi^2} \frac{em_N^2}{a_1^{NLO}(4\pi f_\pi)^2} \left[2h_A^{(2)} + g_A \left(h_V^{(0)} + \frac{4}{3}h_V^{(2)} \right) \right]. \quad (22)$$

Again, using the estimated form factor (21) we have

$$\langle r_1^2 \rangle^{NLO} \simeq s \frac{6}{10m_\pi^2} \ln^{-1} \left(\frac{\mu}{m_\pi} \right)^2. \quad (23)$$

For $\mu = \Lambda_{\chi SB}$ one obtains $\langle r_1^2 \rangle^{NLO} = s(370 \text{ MeV})^{-2}$ and for $\mu = 550 \text{ MeV}$, $\langle r_1^2 \rangle^{NLO} = s(298 \text{ MeV})^{-2}$, where $s = \pm 1$.

We have thus for the first time calculated the momentum dependence of the anapole form factor in next-to-leading order in ChPT. Using dimensional analysis to estimate currently unknown parameters, we see that the variation with momentum is $\sim 20\%$ at $Q \sim 300 \text{ MeV}$ in both isoscalar and isovector channels. The overall size of the anapole contribution to electron scattering is thus likely not very different than that given by the anapole moment itself. We can compare our result for the isovector component to the forthcoming SAMPLE measurement. The SAMPLE collaboration will extract an axial contribution as seen by the electron, $G_A^e(0.1 \text{ MeV}^2)$ [7]. If this value is very different from the tree-level result, it can only be assigned to the anapole form factor if the parameters are substantially larger than the naive dimensional expectation. Using our previous estimate,

$$2h_A^{(2)} + g_A \left(h_V^{(0)} + \frac{4}{3}h_V^{(2)} \right) = -\frac{6G_F(4\pi f_\pi)^2}{\eta F_A^{(1)}(Q^2)} \ln^{-1} \left(\frac{\Lambda_{\chi SB}}{m_\pi} \right)^2 [G_A^e(Q^2) + G_A(Q^2) - G_A^s(Q^2)], \quad (24)$$

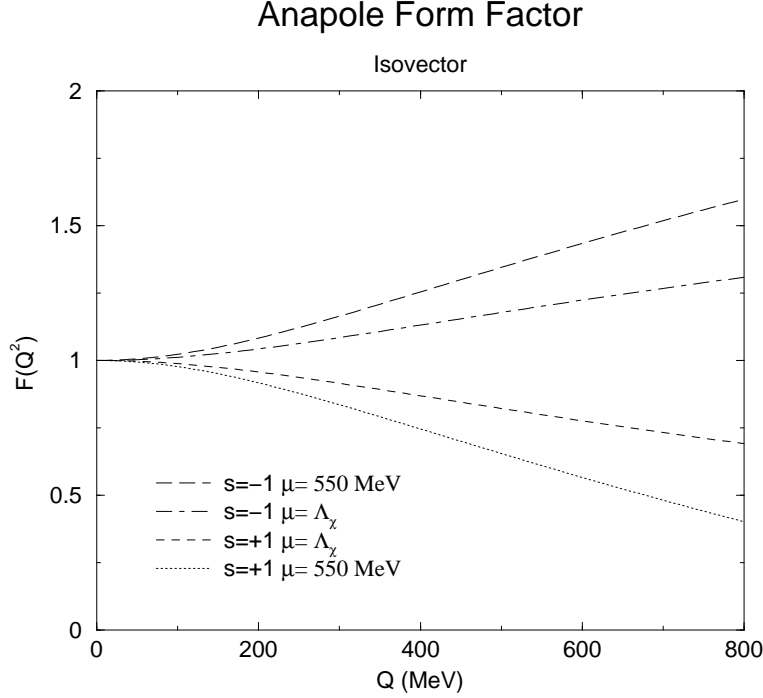


Figure 6: The isovector anapole form factor F_1^{NLO} as function of Q in ChPT, for a few reasonable values of parameters expressed by the regularization scale μ that parametrizes the size of the counterterm, and by s that states the sign of the counterterm.

where $\eta = 8\sqrt{2}\pi\alpha/(1 - 4\sin^2\theta_W) = 3.45$, $G_A(0) = 1.267$, $G_A^s(0) = -0.12$, $G_A(Q^2) = G_A(0)/D(Q^2)$, $G_A^s(Q^2) = G_A^s(0)/D(Q^2)$, $D(Q^2) = 1 + Q^2/M_A^2$, and $M_A = 1.061$ GeV. For example, $G_A^e(0.1\text{MeV}^2) \sim 0.25$ requires $2h_A^{(2)} + g_A(h_V^{(0)} + \frac{4}{3}h_V^{(0)}) \sim -10^{-5}$, a hundred times larger in magnitude than dimensional analysis estimate. This is very unlikely, especially considering a recent estimate in the chiral quark model [16].

In any case, in the future, when parity-violating pion-nucleon parameters are determined from other processes, one can use the results reported here to make firmer predictions for the anapole contribution at various transferred momenta.

Acknowledgements

We thank Bob McKeown and the group at the Kellogg Lab for getting us interested in this problem, and Mike Musolf for discussions. CMM and JSV acknowledge fellowships from FAPESP (Brazil), grants 99/00080-5 and 99/05388-8. This research was supported in part by the US National Science Foundation.

References

- [1] D.T. Spayde et al. (SAMPLE Collaboration), *Phys. Rev. Lett.* **84** (2000) 1106; B. Mueller et al. (SAMPLE Collaboration), *Phys. Rev. Lett.* **84** (1997) 3824.
- [2] E. Beise and M. Pitt (co-spokesperson), MIT-Bates experiment 94-11 .
- [3] Ya.B. Zel'dovich, *Sov. Phys. JETP* **6** (1958) 1184; *Sov. Phys. JETP* **12** (1961) 777.
- [4] C.S. Wood et al., *Science* **275** (1997) 1759.
- [5] M.J. Musolf and B.R. Holstein, *Phys. Rev.* **D43** (1991) 2953; W.C. Haxton, E.M. Henley, and M.J. Musolf, *Phys. Rev. Lett.* **63** (1989) 949.
- [6] D.B. Kaplan and M.J. Savage, *Nucl. Phys.* **A556** (1993) 653.
- [7] R.D. McKeown, in *Parity Violation in Atoms and Polarized Electron Scattering*, ed. by B. Frois and M.A. Bouchiat, World Scientific (1999), p. 423.
- [8] K.A. Aniol et al. (Happex Collaboration), *Phys. Rev. Lett.* **82** (1999) 1096.
- [9] G0 Collaboration, www.npl.uiuc.edu/exp/G0/G0Main.html.
- [10] T.M. Ito (Spokesperson), MIT-Bates experiment 00-004.
- [11] V. Bernard, N. Kaiser, and U.-G. Meißner, *Int. J. Mod. Phys.* **E4** (1995) 193.
- [12] U. van Kolck, *Prog. Part. Nucl. Phys.* **43** (1999) 337.
- [13] S.L. Zhu, S.J. Puglia, B.R. Holstein, M.J.R. Musolf, [hep-ph/0002252](http://arxiv.org/abs/hep-ph/0002252).
- [14] M.J. Savage and R.P. Springer, [nuc1-th/9907069](http://arxiv.org/abs/nuc1-th/9907069).
- [15] C.M. Maekawa and U. van Kolck, *Phys. Lett.* **B478** (2000) 73.
- [16] D.O. Riska, [hep-ph/0003132](http://arxiv.org/abs/hep-ph/0003132).